

1       **The role of references and the elusive nature of the chemical bond**

2                                    Ángel Martín Pendás\* and Evelio Francisco

3       *Depto. Química Física y Analítica. Universidad de Oviedo. 33006 Oviedo, Spain.*

4                                   (\*Electronic address: ampendas@uniovi.es)

5                                   (Dated: April 7, 2022)

**Abstract**

6       Chemical bonding theory is of utmost importance to chemistry. We argue that there is still plenty of  
7       unexplored territory, and that both internal and external reference biases remain in the standard model of  
8       the chemical bond. The former affect the basic notion of wavefunction interference, which is purportedly  
9       recognized as the most basic bonding mechanism. The latter influence how bonding models are chosen.  
10      After unveiling these different biases, we advocate for the use of real space analyses, which are as reference-  
11      less as possible. Delocalisation emerges as the reference-less equivalent to interference and the ultimate root  
12      of bonding. Atoms (or fragments) in molecules should be understood as a statistical mixture of components  
13      differing in electron number, spin, etc.

14 Coinciding with the centennial commemoration of the electron-pair bond proposed by Gilbert  
15 Newton Lewis in 1916,<sup>1</sup> a considerable number of research papers,<sup>2,3</sup> perspective articles<sup>4-6</sup> and  
16 books,<sup>7,8</sup> all revisiting the nature of the chemical bond, have appeared in the literature, showing  
17 the vitality of the field. Most of these recent accounts<sup>4</sup> agree upon the framework forged by K.  
18 Ruedenberg and coworkers in the early 1960's. Following Hellmann's suggestion,<sup>9,10</sup> this *stan-*  
19 *dard model* identifies the kinetic energy lowering suffered by the interacting moieties, triggered  
20 by *constructive interference* of their wavefunctions, with the driving force behind bond formation.  
21 This view opposes that of Slater,<sup>11</sup> who used the virial theorem to vindicate the role of the potential  
22 energy and the accumulation of electron density in the internuclear region upon bonding, and also  
23 in part that of Feynman<sup>12</sup>, who developed an image of bonding in terms of electrostatic forces. As  
24 Frenking and coworkers have emphasized,<sup>4</sup> it is essential that on top of this well accepted phys-  
25 ical image we build *chemical bonding models* that translate the physical language into the fuzzy,  
26 but predictive, chemical concepts. Although different schools still diverge on how fine details are  
27 interpreted and, for instance, valence bond (VB) advocates frequently collide with pure molecular  
28 orbital (MO) practitioners (see, e.g. Refs. 13-15 for recent controversies), a minimal set of points,  
29 that include Hellmann's and Ruedenberg quantum mechanical interference, seems to have been  
30 agreed upon. Interestingly, much of these apparently undisputed core is still not found in general  
31 chemistry textbooks. We show that even these accepted points necessarily imply the choice of both  
32 internal (state) or external (energetic) references which bias interpretations, and propose that the  
33 consideration of interacting atoms or molecules as objects in real space minimizes the reference  
34 bias. Electron delocalisation underpins chemical bonding.

## 35 **Results and Discussions**

36 Ruedenberg and coworkers<sup>7,16,17</sup> have pointed out that building a theory of chemical bonding  
37 requires as a first, absolutely necessary prerequisite to postulate that atoms, or larger entities if  
38 necessary, are somehow preserved in molecules. Chemical bonds occur among interacting moi-  
39 eties that we must single out from the final stable or metastable molecular arrangements. Since  
40 quantum mechanics is an intrinsically non-separable theory, how these atoms are introduced and  
41 manipulated provides a very first source of bias.

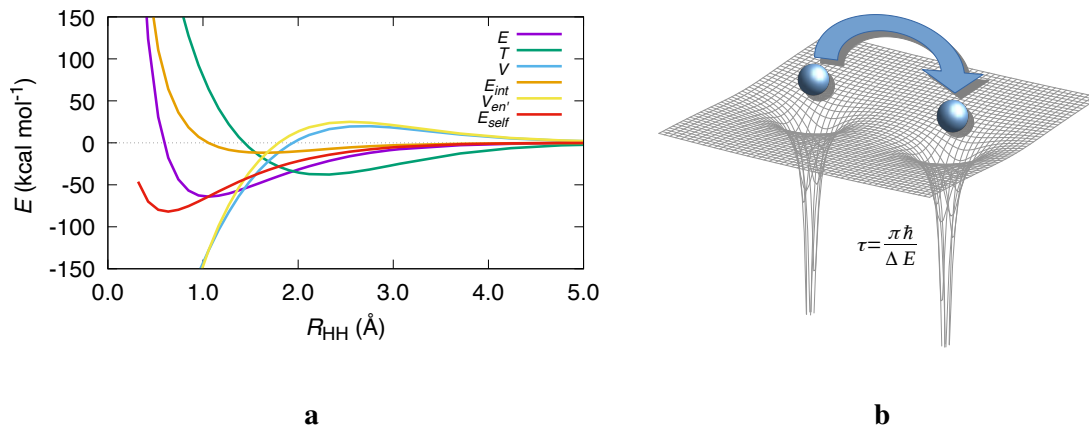


FIG. 1: **Bonding in  $\text{H}_2^+$** . **(a)** FCI cc-pVTZ potential energy curve of  $\text{H}_2^+$  along with several of the energetic descriptors obtained by decomposing the space in two symmetric regions associated to the  $a$  and  $b$  nuclei. All energies referred to their infinite distance limit, in au.  $E_{int}$  is the sum of the internuclear repulsion energy and the attraction energy of the electron density contained in the  $a$  region with the  $b$  nucleus, and vice versa. Similarly,  $V_{en'}$  is the sum of the attraction energy between the electron density in  $a$  with nucleus  $a$  and its  $b$  equivalent. Finally,  $E_{self}$  is the sum of the self-energies of the two regions, see the text, where it is also explained that in the broken symmetry spatial interpretation,  $V_{en'}$  and  $E_{self}$  can also be interpreted as those of a non-entangled H atom interacting with a proton. **(b)** Illustration of Feynman's dynamic picture of the  $2c,1e$  bond.

## 42 The wavefunction reference bias in the $\text{H}_2^+$ molecular ion

43 Take the simplest one electron  $\text{H}_2^+$  ion, described under the clamped-nuclei approximation by  
 44 a wavefunction  $\Psi$ .<sup>18</sup> Fig. 1 shows a potential energy curve with several energetic decompositions  
 45 that will be used in the following. Ruedenberg's variational reasoning is relentless. To lower its  
 46 energy, the electron thrives to balance the opposing kinetic and potential energy demands. The  
 47 first is lowered with electron *delocalisation* or dilution, while the latter becomes more negative  
 48 with *localisation* around the nuclei. The electron is thus pulled towards the nuclei as much as the  
 49 kinetic resistance (also called kinetic pressure) allows. Kinetic ( $T$ ) and potential energy ( $V$ ) low-  
 50 ering dominate the long and short range behavior, respectively and, at equilibrium, the variational  
 51 balance leads to fulfillment of the virial theorem, and  $E = -T$ .

52 *Further chemical analysis requires establishing a reference*, which is standardly taken as the  
 53 H atom and its exact one-electron states (Supplementary Discussion 1), and the molecular wave-  
 54 function is recast in terms of a set of so-called quasi atomic orbitals (QUAOs,  $\phi_{a,b}$ ), which are

55 then compared to the isolated  $\phi_{1s}$  function and used to provide an exact energy and density de-  
 56 composition. Squaring the  $\Psi$  amplitude leads to a sum of the squares of the quasi atomic densities  
 57 and to an *interference* term:  $\rho = \phi_a^2 + \phi_b^2 + \rho_I$ . It is found that the QUAOs pass from slight ex-  
 58 pansion at large  $R$  to significant contraction at equilibrium, and that it is only the interference  $T_I$   
 59 lowering which drives the system to an equilibrium geometry, the accumulation of density in the  
 60 internuclear region being also entirely caused by interference. In this standard model, it is the con-  
 61 structive interference of the atomic functions that allow the electron to dilute or delocalize. Many  
 62 researchers have contributed to the details of this image over the years.<sup>19–24</sup>

63 What is not usually contemplated in general treatments is: (i) that the correct  $R \rightarrow \infty$  asymptotic  
 64 reference of  $\text{H}_2^+$  is a spatially entangled state and not the broken symmetry  $\text{H} + \text{H}^+$  one, (ii) that the  
 65 analysis of the effect of interference depends on spatially separated basis functions, introducing  
 66 completely spurious two-centre terms in an otherwise one-particle problem. As the first point is  
 67 regarded, it is all but clear that the infinite distance asymptotic wavefunction  $\Psi = 1/\sqrt{2}(\phi_{1sa} +$   
 68  $\phi_{1sb})$  describes an entangled electron with a 50% probability of being found around each nucleus,  
 69  $p(n_a = 1, n_b = 0) = p(n_a = 0, n_b = 1) = 1/2$ , and not a H atom and a proton,  $p(n_a = 1, n_b =$   
 70  $0) = 1, p(n_a = 0, n_b = 1) = 0$ . This takes us to R. Feynman,<sup>25</sup> who interpreted the  $\text{H}_2^+$  system in  
 71 terms of the dynamic flip-flop jump of the electron between the two atomic regions (Fig. 1, right  
 72 panel). In the long distance limit a state that is initially described by the localized  $\phi_a$  function will  
 73 tunnel to  $\phi_b$  with a rate  $\tau = (\pi\hbar)/\Delta E$ , where  $\Delta E$  is the system's first excitation energy. As distance  
 74 increases and  $\Delta E$  tends to zero, the tunneling time grows indefinitely. This dynamic picture has  
 75 been exploited over the years by Nordhom and Backsay,<sup>26,27</sup> among others.

76 As it stands out, *interference is an a posteriori result of the wavefunction decomposition, not*  
 77 *an intrinsic feature of the system.*  $\text{H}_2^+$  is a problem of a particle moving in a potential  $V(\mathbf{r})$ .  
 78 Isolating two wells (the two nuclei) is necessary for chemical analyses, but alien to the physics  
 79 of the problem. Let us consider a textbook one-dimensional particle moving in a box of length  $L$   
 80 resulting from the interpenetration of two smaller left and right boxes of length  $2/3L$ , which we  
 81 label  $a$  and  $b$  (see Fig. 2). After eliminating the right- $a$  and left- $b$  *constraining* walls (dashed lines  
 82 at  $2L/3$  and  $L/3$ , respectively), we build an approximation to the solutions of the larger box in  
 83 terms of those of the original  $a$  and  $b$  problems. With the sinusoidal ground states  $\phi_a, \phi_b$  of the  
 84 initial boxes we can approximate the ground state of the final system as  $\Psi = N(\phi_a + \phi_b)$ . The  
 85 ground state of the large box can be recast as the constructive combination of two symmetric,  
 86 deformed solutions of the  $a, b$  boxes. For an observer unaware of our gedanken small boxes,

87 using the solutions of these two hidden ancillary systems is a completely arbitrary process, as it is  
 88 assigning any physical sense to the constructive interference of  $\phi_a$  and  $\phi_b$ . *This internal bias soaks*  
 89 *the standard model of chemical bonding*. As  $V = 0$  inside the box,  $E = T$ , and it suffices to consider  
 90  $\hat{T} = -(1/2)d^2/dx^2$ . All the following considerations apply also to  $V$  when it is non-vanishing.  
 91 Recall that (in atomic units) the energy of the ground state of an electron in a box of size  $L$  is  
 92  $\pi^2/(2L^2)$ . By releasing the right-wall constraint at  $2L/3$  of an electron initially confined in the left  
 93  $a$  box and letting it occupy the  $a \cup b$  larger box,  $E = T$  decreases. The role of the release of spatial  
 94 constraints in chemical bonding has been put forward several times,<sup>27</sup> and in our opinion is the true  
 95 core upon which all chemical bonding treatments rest. In terms of interference,  $T = T_a + T_b + T_I$   
 96 where  $T_I = -(1/2) \int_0^L \phi_a(x)(d^2\phi_b(x)/dx^2) dx$ . Notice that in  $H_2^+$   $T_I$  is interpreted as an *interatomic*  
 97 term. This is an *artifact* coming from the mixing of  $\phi_a$  and  $\phi_b$ .  $T$  is a one-particle, *thus one-centre*  
 98 observable. For the final ground state,  $T = (-1/2) \int_0^L \Psi(x)(d^2\Psi(x)/dx^2) dx$ , and no two-centre  
 99 contributions arise. It is only when we decompose  $\Psi(x)$  at point  $x$  into two contributions assigned  
 100 to two different centres that an inter-centre *interference* term appears. We conclude that *two-*  
 101 *centre contributions for one-particle operators should be avoided to by-pass internal or state*  
 102 *reference biases*. They should only be present when considering the interelectron repulsion, a  
 103 true two-particle operator that can display two-centre behavior. Fig. 2 helps us envisage how we  
 104 can still associate the particle to two centres (boxes) without invoking any internal reference or  
 105 interference term. Since the initial limits of the boxes disappear when the wall constraints are  
 106 released, a reasonable assumption follows: if the electron is in the left/right region of the final  
 107 box we associate it to the remnants of the left/right initial boxes. Symmetry arguments put the  
 108 separation of the in-the-molecule left and right regions at the short-dash orange line in the Figure.  
 109 A natural *spatial partitioning* that divides space into (chemically) relevant regions appears.

110 No internal reference or arbitrary choice remains at all. In more general cases, a choice about  
 111 how the spatial partitioning is performed is needed, but the number of degrees of freedom for  
 112 this decision is much smaller than in other cases. The spatial partition leads to a probability of  
 113 finding the electron in each of the boxes-in-the-box equal to  $1/2$ , and to a regional kinetic energy  
 114  $T^{a,b} = T/2$ . We can still use the original  $a, b$  boxes as references, and compute the changes in  $T^a$   
 115 on going from the isolated  $a$  box to the  $a$  box-in-the-box situation. This is the basis of real space  
 116 bonding analyses. In this view, an electron found in a given (chemical) region is *never* considered  
 117 part of another one, as when interpenetration is allowed.

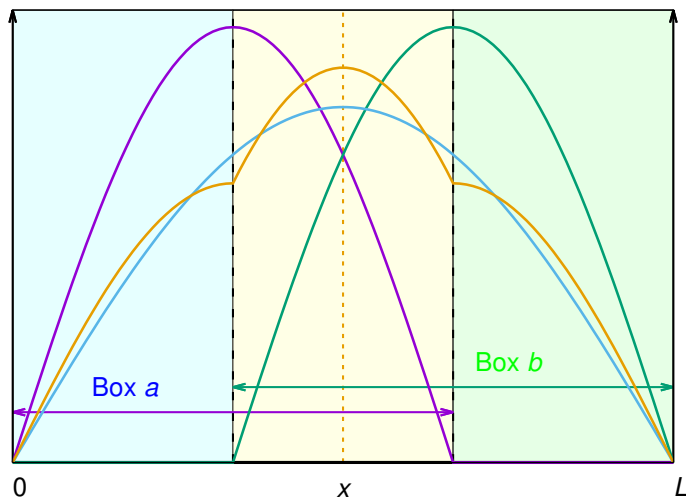


FIG. 2: **A model for the wavefunction reference bias.** A one-electron one-dimensional box of length  $L$  built from the interpenetration of two smaller left ( $a$ , blue) and right ( $b$ , green) boxes of length  $2/3L$ . The interpenetration region is depicted in yellow. The ground states of an electron initially confined in either the  $a$  or  $b$  boxes,  $\phi_a, \phi_b$  are shown as the purple and green solid curves. If the impermeable walls (long-dashed lines) are released, the electron delocalizes, and its ground state,  $\Psi$  is depicted in cyan. When  $\Psi$  is approximated by the gerade linear combination of  $\phi_a$  and  $\phi_b$ ,  $\Psi = N(\phi_a + \phi_b)$ , in orange,  $S_{ab} \approx 0.2153$ . The spatial partitioning of the large box into two equivalent non-interpenetrating regions of length  $L/2$  is depicted by the short-dashed orange line.

118 *The real space image*

119 A spatial partitioning of the entangled ground state of  $\text{H}_2^+$  leads to a 50% probability of the  
 120 electron being found in any of the two atomic regions (i.e. basins), at any distance:  $p(n_a = 1, n_b =$   
 121  $0) = p(n_a = 0, n_b = 1) = 1/2 = \int_a \rho(\mathbf{r}) d\mathbf{r}$ . All kinetic and electron-nuclear potential energy  
 122 terms can be decomposed into basin contributions:  $T = T^a + T^b$ ,  $V_{en} = V_{en}^{aa} + V_{en}^{ba} + V_{en}^{ab} + V_{en}^{bb}$ ,  
 123 with  $V_{en}^{ab}$  being, for instance, the electron-nucleus ( $en$ ) attraction between the electron, when it  
 124 is contained in region  $a$ , and nucleus  $b$ . There are powerful reasons to choose the atomic basins  
 125 provided by the quantum theory of atoms in molecules (QTAIM)<sup>28</sup>, a standard which we will  
 126 follow. The sum of  $T_a + V_{ne}^{aa}$  corresponds to the energy of the electron residing in atom  $a$ , that  
 127 is usually called its self-energy,  $E_{self}^a$ . In polyelectronic cases it also includes the interelectron  
 128 repulsion of the electrons located in  $a$ ,  $V_{ee}^{aa}$ . Similarly, the sum  $E_{int}^{ab} = V_{en}^{ab} + V_{en}^{ba} + 1/R_{ab}$  (with an  
 129 additional polyelectronic  $V_{ee}^{ab}$  repulsion if needed) is the interaction of the electron when residing

130 in a basin with the other nucleus and vice versa, plus the internuclear repulsion  $V_{nn}^{ab} = 1/R_{ab}$ . It  
 131 is called the interatomic interaction energy. Adding up,  $E = E_{self}^a + E_{self}^b + E_{int}^{ab}$ . This is the so-  
 132 called interacting quantum atoms (IQA) energy decomposition.<sup>29–31</sup> All of these components can  
 133 be found in Fig. 1 (Supplementary Discussions 2, 3), where  $V_{en}^{aa} + V_{en}^{bb}$  is called  $V_{en'}$ .  $E_{self}^a$  tends  
 134 to  $-1/4$  au at dissociation, which is obviously equal to  $p(1,0) \times E(\text{H}) + p(0,1) \times E(\text{H}^+)$ .  $E_{self}^a$   
 135 is stabilized as  $R$  decreases, contrarily to its equivalent  $E_{intra}$  in Ruedenberg’s analysis, since the  
 136 strongly stabilizing interference kinetic energy  $T_I$  of the latter is now an intra-basin phenomenon.  
 137 Interestingly, even though no atomic functions are used in this real space analysis, orbital-like  
 138 expansion and contraction can be easily recognized from how  $V_{en}^{aa}$  (or  $V_{en'}$  in the Figure) changes  
 139 with respect to their values at dissociation. This change is initially positive to become negative  
 140 as  $R$  decreases. The contrary is true for  $\Delta T^a$ . Notice also how  $V$  differs only slightly from  $V_{en'}$   
 141 for a wide range of distances. The real space viewpoint unveils the release of constraints, thus  
 142 *delocalisation*, as the ultimate root of chemical binding. If we confine the electron to either the  
 143 left or right basins, variational reasoning leads to  $E_{self}^a > E(\text{H})$  at any distance. Once electron  
 144 delocalisation (basin hopping á la Feynman) is allowed, chemical bonding sets in. The real space  
 145 analysis also permits a broken symmetry perspective (Supplementary Discussion 2).

146 The evolution of one-electron bonds towards polarity can be followed in the alkali dimer  
 147 cations,  $\text{AB}^+$ , which are well modeled by a 2c,1e paradigm. A single reference (SR) wavefunction  
 148 for  $\text{LiNa}^+$  leads to  $p(n_{\text{Li}} = 3, n_{\text{Na}} = 10) = 0.748$ ,  $p(2, 11) = 0.251$ , with a residual contribution for  
 149 other electron counts: a polar 2c,1e bond where the electron has 25% probability of being found in  
 150 the Na atom. Manipulating the difference of electronegativities between the atoms induces a shift  
 151 from the (close to) perfect non-polar 2c,1e bond in  $\text{Li}_2^+$  with  $p = 1/2$ , passing through  $p \approx 0.75$  in  
 152  $\text{LiNa}^+$ , towards  $p \approx 1$  in  $\text{LiCs}^+$ .

## 153 The $\text{H}_2$ molecule

154 Adding a second electron to the  $\text{H}_2^+$  system leads to the electron-pair bond. As in  $\text{H}_2^+$ , it is the  
 155 kinetic energy interference term,  $T_I$ , which drives bonding in the standard model. Nevertheless,  
 156 a couple of new insights, which are usually hidden or not fully considered, stand out: (i) An  
 157 important contribution to the interatomic potential, the so-called *coulombic sharing*<sup>32</sup> term appears  
 158 because of the existence of intra-atomic electron-electron repulsion. (ii) The electron-pair bond is  
 159 not a result of electron spin pairing. Actually, the binding energy of dihydrogen is smaller than

twice that of  $\text{H}_2^+$  (109.5 *versus* 64.4 kcal mol<sup>-1</sup>),<sup>33</sup> and  $\text{H}_2$  should be viewed as two independent two-centre one-electron bonds, slightly weakened by the interelectron repulsion that is absent in  $\text{H}_2^+$ .<sup>4</sup> According to Ruedenberg and coworkers, this picture is general, and kinetic interference is the root of all bonding. Head-Gordon *et al*<sup>34–36</sup> have questioned this view, pointing to electron delocalisation as the most general bonding driver.

In the real space picture of  $\text{H}_2$ ,<sup>29</sup> the spatial regions associated to the H atoms are symmetry determined. The self-energy of each atom,  $E_{self}^{a,b}$ , increases upon molecular formation, so that all binding comes from  $E_{int}^{ab}$ , which is naturally decomposed into a repulsive ionic  $V_{cl}^{ab}$  term (net charge dominated) and an attractive covalent-like  $V_{xc}^{ab}$  (exchange-correlation) one, see Supplementary Discussion 2. A vital point stands out: *the two electrons can be both found in one of the two atoms a or b*. Atoms in molecules should not be imagined possessing a fixed number of electrons. If this is done, we face *an electron number bias*, for we must choose arbitrarily the number of electrons of our references. In  $\text{H}_2$ , three possible electron distributions are possible: (1, 1), (2, 0) and (0, 2), labeled according to the number of electrons in *a* and *b*. The first is compatible with neutral atomic references, while the other two correspond to ionic  $\text{H}^-$  and  $\text{H}^+$  ones. An interacting atom or fragment *a* is in a *mixed open quantum state*, with a probability  $p(n_a)$  of being found with a given electron count  $n_a$ . In this view,<sup>37,38</sup>  $E = \sum_i p_i E_i$ . In the simplest MO  $1\sigma_g^2$  wavefunction of  $\text{H}_2$ ,  $p(1, 1) = 1/2$ , and  $p(2, 0) = p(0, 2) = 1/4$  (see Supplementary Discussion 2).<sup>38</sup> This describes two independent 2c,1e  $\text{H}_2^+$ -like bonds, each electron ignoring the other, with a 50% probability of being found in each atom.

The role of correlation is also clear. A multireference (MR) wavefunction in  $\text{H}_2$ <sup>39</sup> shows that  $p(1, 1) = 0.584$ ,  $p(2, 0) = p(0, 2) = 0.208$  at  $R = 1.4$  au, corroborating that electron correlation decreases delocalisation and increases the probability of finding each of the two electrons closer to the (different) nuclei. As  $R$  increases,  $p(1, 1)$  tends to 1, and at  $R = 6.0$  au, it is equal to 0.988 (full configuration interaction results with larger basis sets<sup>37,40</sup> do not alter this image). The energy of the (1, 1) electron distribution at  $R = 1.4$  au is  $-1.260$  au, with  $E_{self}^a = -0.653$  and  $E_{int}^{ab} = +0.047$  au, respectively. These tend to  $-0.500$  and  $0.000$  au at dissociation, respectively. As the (2, 0) distribution is regarded, at  $R = 1.4$  au  $E = -0.996$  au, with  $E_{self}^a = -0.496$ ,  $E_{self}^b = 0$ , and  $E_{int}^{ab} = -0.500$  au, respectively. These tend to  $-0.467$  (the energy of a hydride anion at the single-determinant level with the chosen basis set) and  $0.000$  au, respectively, at dissociation. These numbers show how grossly incorrect choosing references with fixed number of electrons can be. In each of the (1, 1) or (2, 0)  $\equiv$  (0, 2) distributions a fixed number of electrons reside in each

192 atomic region. When strictly one electron is found in each atom, all the interaction is quasiclassical  
193 (although built with the quantum mechanical density), and an electrostatic theorem<sup>41</sup> guarantees  
194 that their interaction is repulsive. In agreement with the standard (i.e. Ruedenberg) model, the very  
195 negative (1,1)  $E_{self}$ 's imply a highly contracted electron density. Contrarily, for the (2,0) H<sup>-</sup>-  
196 H<sup>+</sup> distribution  $E_{int}$  is large and negative, behaving as  $-1/R$  asymptotically, while  $E_{self}^{H^-}$  reveals a  
197 slightly contracted hydride. If delocalisation is prohibited,<sup>42</sup> the (1,1) distribution would lead to a  
198 repulsive potential energy curve, for a minimisation of the (1,1) energy would lead to  $E_{self}^a > E^H$   
199 (and  $E_{int}^{ab} > 0$ ).

200 Summarizing: (i) Associating interference as the driving force behind chemical bonding is, to  
201 a large extent, the result of assuming a set of internal references. Since it needs not be imposed,  
202 it cannot be taken as the final root of the chemical bond, which we ascribe to delocalisation in  
203 its most general sense; (ii) Even for the simplest dihydrogen case, the consideration of a neutral  
204 reference disregards the fact that at equilibrium about half the time one of the H atoms bears two  
205 electrons.

## 206 The energy reference bias

207 Out of the many energy decompositions in the literature, Ziegler and Rauk's EDA,<sup>43</sup> many  
208 times in combination with the natural orbital for chemical valence (NOCV) analysis<sup>44</sup> has proven  
209 useful in building chemical bonding models. We use it here for illustrative purposes. Its basic  
210 tenet is that building a chemical bonding model needs (at least) two fragments that interact, from  
211 which we measure or compute changes. These fragments are isolated at the equilibrium geome-  
212 try of the molecule, and their electronic structure is determined in electronic states that may not  
213 coincide with their ground state, but that have chemical sense (*vide infra*). Then, their interaction  
214 energy  $\Delta E_{int}$  is determined through a sequence of steps: (i) the classical electrostatic interaction  
215 between their total (nuclear and electronic) interpenetrating charge densities,  $\Delta E_{elstat}$  is deter-  
216 mined. This is typically stabilizing, and EDA-NOCV advocates have emphasized the role of these  
217 *forgotten* quasi-electrostatic terms in bonding.<sup>5</sup> (ii) The frozen fragments' wavefunctions are anti-  
218 symmetrized, and the concomitant rise in energy is associated to the Pauli repulsion  $\Delta E_{Pauli}$  among  
219 the non-relaxed electrons of the fragments; (iii) Finally, the antisymmetrized function is orbitally  
220 relaxed (i.e. a full calculation is done in the molecule). The energy drop is the orbital relaxation en-  
221 ergy,  $\Delta E_{orb}$ , which is linked to covalency. In the end,  $\Delta E_{int} = \Delta E_{elstat} + \Delta E_{Pauli} + \Delta E_{orb}$ . If needed,

222 a dispersion contribution,  $\Delta E_{disp}$  is also added. When the geometries, electronic or spin states of  
223 the fragments do not coincide with those at dissociation, another term, the preparation energy,  
224  $\Delta E_{prep}$ , is necessary, so that  $\Delta E = -D_e = \Delta E_{prep} + \Delta E_{int}$ . The application of this EDA is not al-  
225 ways viable: it requires final single determinant descriptions (or Kohn-Sham quasi-determinants),  
226 it has problems with metastable or high energy content molecules that display exothermic dissoci-  
227 ations, and it sometimes requires tricks to build the appropriate molecular spin state from those of  
228 the fragments.

### 229 **Intrinsic bond strength and metastable bonds**

230 Given that  $D_e$  includes  $\Delta E_{prep}$  that can mask bonding effects, it has been suggested<sup>2</sup> that it  
231 is  $\Delta E_{int}$  that provides a faithful descriptor of the intrinsic bond strength, the chemically relevant  
232 bond energy. Since this is obviously a troublesome indicator (e.g. in metastable molecules),  
233 many researchers, pioneered by Cremer and Kraka,<sup>45</sup> prefer to abandon energies to measure bond  
234 strength and to turn to local measures, independent of references, such as local force constants.  
235 Although these are not uniquely defined, they have considerable advantages, and have been re-  
236 cently advocated by Zhao *et al* as a solution to the bond dissociation energy (BDE) conundrum.<sup>46</sup>  
237 It has also been suggested that reference-less real space  $E_{int}$ 's can be used as *in situ* bond strength  
238 parameters.<sup>47</sup> We take as an example the  $\text{He}_2^{2+}$  system. This is a metastable two-electron ion. A  
239 MR calculation yields a metastable minimum at  $R = 1.332$  au,  $201.2$  kcal mol<sup>-1</sup> above the dis-  
240 sociation limit. The well is about  $34$  kcal mol<sup>-1</sup> deep, with a very large force constant of  $12.51$   
241 mdyn Å<sup>-1</sup>, larger than in dihydrogen,  $5.55$  mdyn Å<sup>-1</sup>.<sup>48</sup> A real space partition at the metastable  
242 minimum yields a simple  $2c, 2e$  close to that in  $\text{H}_2$ :  $p(1, 1) = 0.617$ , with a covalent bond order of  
243  $0.765$ .  $E_{int} = +266.4$  kcal mol<sup>-1</sup>, partitioned into  $462.2$  kcal mol<sup>-1</sup> electrostatic destabilisation  
244 between the  $\text{He}^+$  cations (the pure Coulombic repulsion between two unit point charges at that  
245 distance is  $471.1$  kcal mol<sup>-1</sup>) and  $-195.8$  kcal mol<sup>-1</sup> exchange-correlation stabilisation (Sup-  
246plementary Discussion 3). The covalent component in dihydrogen is smaller, around  $-149$  kcal  
247 mol<sup>-1</sup>. Applying the EDA prescription to a single-determinant wavefunction obtained at the FCI  
248 geometry with  $\text{He}^+$  references we obtain (all data in kcal mol<sup>-1</sup>)  $\Delta E_{elstat} = 474.3$ ,  $\Delta E_{Pauli} = 0$ ,  
249  $\Delta E_{orb} = -229.5$ . Since in a  $2e$  singlet the EDA Pauli repulsion vanishes,  $\Delta E_{orb}$  can be rather  
250 safely associated with the onset of covalency. The reference-less  $E_{int}^{ab}$  together with its ionic and  
251 covalent components provide local energetic information about bond strength that can be used on

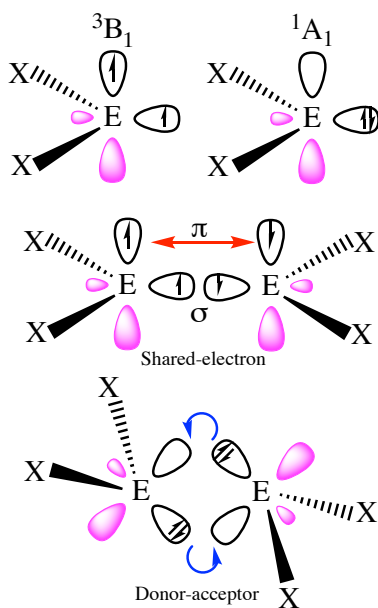


FIG. 3: **Transition from shared-electron to donor-acceptor chemical bonding models in  $E_2X_4$  systems.**

If fragments interact in their ground state throughout the full association path, planar or trans-bent geometries are expected for triplet or singlet  $EX_2$ 's, respectively. In the case of small singlet-triplet promotion energies, the bonding mode can change along the association, as in  $C_2F_4$ .

252 a par with local force constants.

### 253 **Chemical bonding models from energy references**

254 Frenking and coworkers<sup>5</sup> have shown how to make the most of the *a priori* freedom to choose  
 255 the electronic/spin states of the fragments. According to their protocol, different references cor-  
 256 respond to different bonding models, and a variational-like argument is used to select the most  
 257 appropriate fragment choice: the preferred model is that displaying the smallest  $\Delta E_{orb}$  step, with  
 258 fragments as prepared as possible for bonding to take place. There exist many successful examples  
 259 of this approach. It allows to rationalize the planar and trans-bent geometries of  $C_2H_4$  and  $Si_2H_4$ ,  
 260 respectively, and of many other  $E_2X_4$  heavy molecules (see Fig. 3). The  $CH_2$  fragments' ground  
 261 state is a  $^3B_1$  triplet, with two unpaired electrons perfectly suited to engage in a double bond. On  
 262 the contrary, the heavier  $EH_2$  fragments are  $^1A_1$  ground state singlets, which have to be formally  
 263 excited to the triplet to get involved in electron-sharing. Thus they prefer donor-acceptor interac-  
 264 tions that lead to non-planar geometries.<sup>2</sup>  $C_2F_4$  is a mostly interesting case: although the isolated  
 265  $CF_2$  fragment is a singlet with a singlet-triplet gap of about  $51.2 \text{ kcal mol}^{-1}$ ,  $\Delta E_{orb}$  is considerably

TABLE I: **Energetic Reference bias in LiF.** HF//def2-SVP EDA analysis with neutral and ionic references. Energies in kcal mol<sup>-1</sup>.

Reference	$\Delta E_{elstat}$	$\Delta E_{Pauli}$	$\Delta E_{orb}$
LiF	-14.26	60.90	-135.85
Li <sup>+</sup> F <sup>-</sup>	-183.83	33.96	-26.62

266 smaller if the EDA fragments are made to interact as triplets,<sup>49</sup> so that the C<sub>2</sub>F<sub>4</sub> ground state is,  
 267 as in ethylene, planar and well described by a double bond. The singlet to triplet excitation cost  
 268 manifests in the very small  $D_e = 74.4$  kcal mol<sup>-1</sup>, much smaller than  $\Delta E_{int} \approx -200$  kcal mol<sup>-1</sup>,  
 269 of a normal C-C double bond. Association of two <sup>1</sup>A<sub>1</sub> CF<sub>2</sub> moieties proceeds via a dative or  
 270 donor-acceptor trans-bent geometry which is progressively planarized: bonding interactions may  
 271 change during bond formation, warning us about using dissociation products as probes for dative  
 272 or electron-sharing interactions.

### 273 *Single reference systems*

274 It is at this point that all our alarms ring together. In order to appropriately use the energetic  
 275 promotion of fragments *during* bond formation one must consider their mixed quantum nature  
 276 and allow for both electron number and electronic/spin state fluctuations. Moreover, electron  
 277 reorganisations along a reaction coordinate more than often require high level quantum mechan-  
 278 ical descriptions beyond single-determinant (including Kohn-Sham) approximations, where most  
 279 EDAs break down. We examine a few illustrative cases. The LiF molecule is a closed-shell system  
 280 very well described at the Hartree-Fock level. Even in a simple SR description, Table I shows that  
 281 the chemical bonding protocol selects the ionic reference. If the neutral fragments are considered  
 282 to engage in electron sharing, a small stabilizing electrostatic energy appears, together with a non-  
 283 negligible Pauli repulsion caused by the overlap of the Li 2s function with the bonding 2p<sub>z</sub> orbital  
 284 of F and a very large orbital stabilisation. This picture is turned upside down if the ionic reference  
 285 is used, which requires an experimental ionisation cost of 45.9 kcal mol<sup>-1</sup>, obtained as the sum  
 286 of the first ionisation energy of Li and the electron affinity of F.<sup>48</sup> Reference-less IQA data lead  
 287 to electrostatic  $V_{cl} = -173.9$  and covalent  $V_{xc} = -32.9$  kcal mol<sup>-1</sup> contributions, respectively, in  
 288 rather good agreement with their EDA equivalents for an ionic reference. This accord is easy to

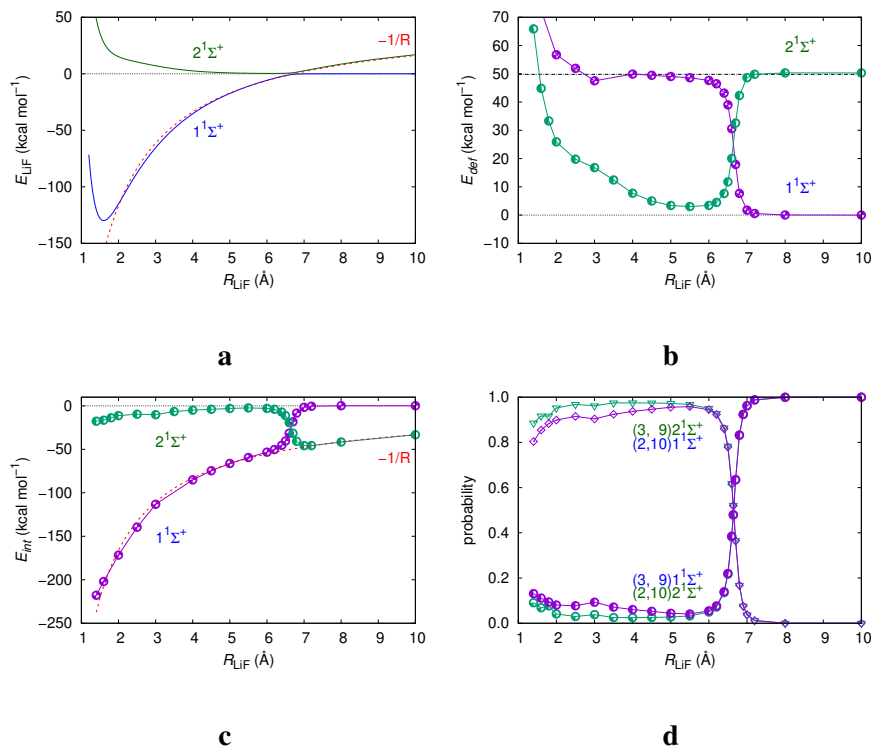


FIG. 4: **Spatial partitioning in LiF.** d-aug-cc-pVDZ MRCI-SD data in both the S0 ( $1^1\Sigma^+$ ) and S1 ( $2^1\Sigma^+$ ) states along the dissociation curve. **(a)** Total energy, showing the avoided crossing. **(b)** Total self-energy ( $E_{self}^{Li} + E_{self}^F$ ). The energy reference is set to the neutral reference, while the ionisation cost of LiF is  $49.5 \text{ kcal mol}^{-1}$ . **(c)** Total  $E_{int}^{LiF}$ , together with the Coulombic  $-1/R$  contribution. **(d)** Probabilities of the main electron distributions.

289 understand if we examine the distribution of electron counts in the LiF atoms:  $p(2, 10) = 0.887$ ,  
 290  $p(3, 9) = 0.095$ ,  $Q(\text{Li}) = +0.910$ . The distribution is overwhelmingly dominated by one electron  
 291 count, and a single (ionic) reference suffices. The EDA protocol works well here only if allow  
 292 non-neutral fragment references, i.e. if we admit the *electron count bias*. Dissociation along the  
 293  $1^1\Sigma^+$  ground state curve leads to neutral fragments through a very well studied multireference  
 294 avoided crossing. Standard EDA cannot be used to follow this change, but a multiconfigurational  
 295 character poses no problem for real space analyses. A MR calculation<sup>50</sup> shows that a tight avoided  
 296 crossing between the S0  $1^1\Sigma^+$  and S1  $2^1\Sigma^+$  states, which become less than  $2 \text{ kcal mol}^{-1}$  apart,  
 297 occurs at  $R \approx 6.6 \text{ \AA}$ . As we decrease  $R$  and pass the avoided crossing, all  $E_{self}$  and  $E_{int}$  compo-  
 298 nents jump suddenly from the values expected for an electron sharing interaction between neutral  
 299 entities to those of an ionic interaction between  $\text{Li}^+$  and  $\text{F}^-$  ions, the contrary being true on the

300  $2^1\Sigma^+$  curve (see Fig. 4 and Supplementary Discussion 4). This violent transition shows how the  
301 chemical bonding between two species can change character abruptly. It is remarkable that from  
302 dissociation down to almost the ground state equilibrium geometry the electron distribution is  
303 dominated by just two components,<sup>51</sup>  $p(n_{\text{Li}} = 3, n_{\text{F}} = 9) = p$  and  $p(n_{\text{Li}} = 2, n_{\text{F}} = 10) \approx 1 - p$ ,  
304 and that their evolution in the S0 state is almost symmetric to that in S1, with  $p_{\text{S0}} \approx 1 - p_{\text{S1}}$ .  
305 At the crossing,  $p$  is 0.5. A crystal clear chemical bonding model emerges: bonding in LiF is  
306 extremely well parametrized by a  $2c, 1e$  bond where the probability of the electron being found  
307 in one or the other atom (à la Feynman) changes from one to almost zero. In this case, the use  
308 of a physical energetic partition applicable during the complete bonding process, both in ground  
309 and excited states, validates the insights obtained from the two-point (equilibrium, dissociation)  
310 EDA protocol. In passing, we comment on the reticence extended among many researchers<sup>2,52</sup>  
311 about the existence of true ionic bonding outside ionic crystals, where ions are lattice-stabilized.  
312 This reluctance is not found among molecular physicists, well acquainted with avoided crossings.  
313 A chemical model of how the ionisation barrier is overcome without a total energy barrier is as  
314 follows: two neutral atoms interact, attracting themselves so that their overall energy decreases.  
315 At about the avoided crossing, the energy of the ionic arrangement competes with the neutral one,  
316 so that the jump occurs in quasi-degeneracy conditions. At equilibrium, almost only one electron  
317 distribution dominates (the ionic one), and a CCSD/aug-cc-pVTZ calculation yields Li,F moieties  
318 with self-energies just 9 and 25 kcal mol<sup>-1</sup> above those of the Li<sup>+</sup> and F<sup>-</sup> ions.<sup>47</sup>

### 319 *Limitations*

320 Let us consider the formation of CH<sub>4</sub> from a C atom and a H<sub>4</sub> fragment, all maintaining tetra-  
321 hedral symmetry. Standard chemical wisdom proposes to promote the C atom to the  $^5\text{S}-2s^12p^3$   
322 state and then to hybridize in order to form four bonds. The two steps need about 96.5 and 62  
323 kcal mol<sup>-1</sup>, respectively.<sup>47</sup> A MR calculation<sup>47</sup> showed that as  $R_{\text{C-H}_4}$  decreases, the probability  
324 of finding six electrons in C (and with it the usefulness of a neutral C reference) also decreases.  
325 At equilibrium,  $p(n_{\text{C}} = 6)$  is about 0.3, and all  $p(n_{\text{C}})$  with  $n_{\text{C}}$  ranging from 2 to 10 are non-  
326 negligible. If only the  $n_{\text{C}} = 6$  components are considered, the weight of a quintet contribution  
327 peaks at a maximum of about 20% at a  $R_{\text{C-H}}$  distance of about 1.9 Å. This makes just a 6% of  
328 all the components. Assuming a fixed electron count for atoms is not justified. At variance with  
329 the avoided crossing case, where one distribution is very quickly changed into another, no abrupt

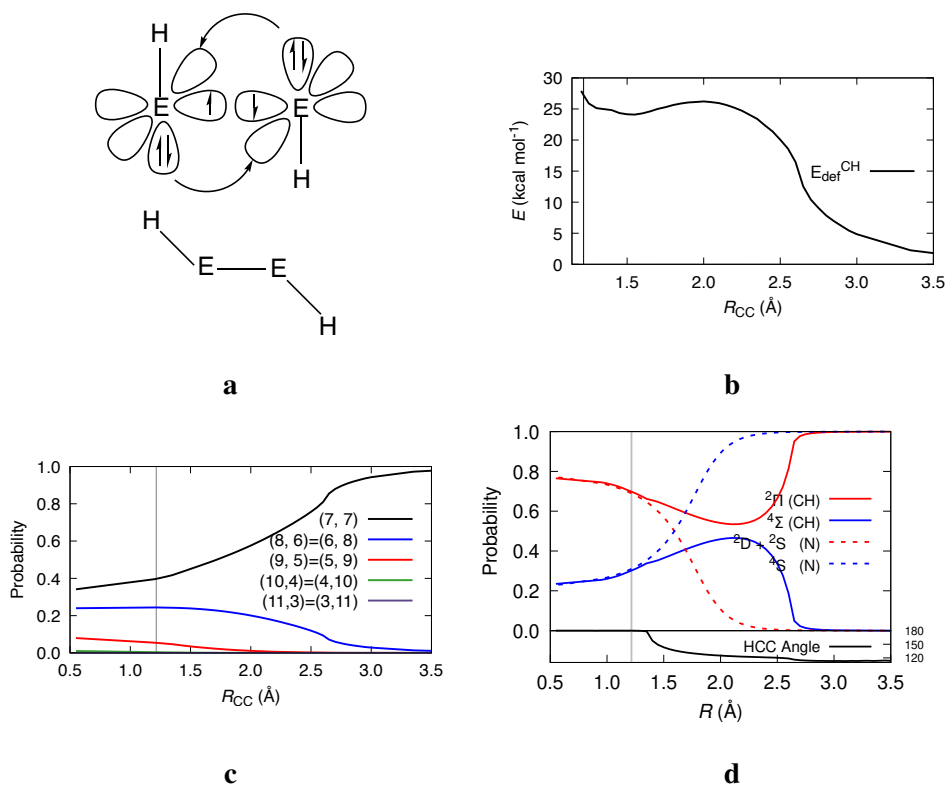


FIG. 5: **Spatial partitioning in acetylene.** CASSCF/def2-TVZPP data along the association process of two ground state  $^2\Pi$  CH fragments to form acetylene. **(a)** Chemical bonding model explaining the trans geometry path. **(b)**  $E_{def}$  of the CH fragment. **(c)** Probabilities of the different electron distributions. **(d)** Normalized probabilities of the spin states of the (7,7) neutral distribution, superimposed on those obtained for  $N_2$  at the same level of theory, and including the variation of the HCC angle along the process. Vertical lines are also drawn at the equilibrium distance.

330 change of any descriptor is found along the ground state energy curve, since the weights of all  
 331 distributions change smoothly. Thus, as the fragments progressively interact and deform,  $\Delta E_{prep}$   
 332 for the statistical mixture of electron distributions and electronic/spin states evolves also smoothly.  
 333 At equilibrium,  $E_{self}^C$  is 62 kcal mol<sup>-1</sup> above the C triplet ground state, which is much lower than  
 334 the expected 158 kcal mol<sup>-1</sup> of the EDA promotion+hybridisation energies. Transit from dis-  
 335 sociation to equilibrium occurs, thanks to statistical mixing, through C atoms that never exhibit  
 336 the full preparation energy of the EDA modeling. The usefulness and predictive ability of the  
 337 EDA protocol is not challenged with this discussion: it is simple and easy to use. We just show  
 338 that reference-less formalisms uncover a more complex reality, and that care should be taken in  
 339 applying EDA blindly.

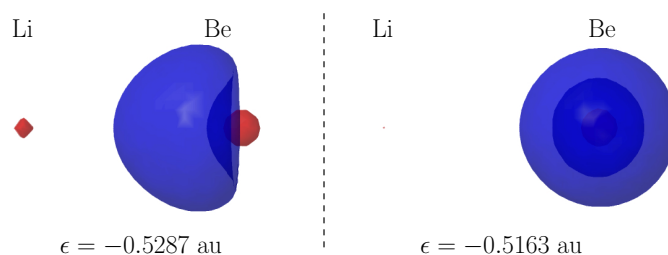


FIG. 6: **Symmetry broken LiBe<sup>+</sup>**. Be 2s-like orbitals in LiBe<sup>+</sup> at the UHF/6-311G(p) level, computed at  $R_{\text{LiBe}} = 2.6 \text{ \AA}$ . Orbital energies are also depicted. Only the left function is actively delocalized over the Li moiety. The isosurfaces shown correspond to  $|\phi| = 0.1 \text{ au}$

340 Another example follows the wake of the C<sub>2</sub>F<sub>4</sub> case: the formation of the triple bond in acetylene  
 341 lene from the interaction of two methyldyne CH radicals, which display <sup>2</sup>Π ground states 17.3  
 342 kcal mol<sup>-1</sup> below <sup>4</sup>Σ<sup>-</sup> quartets. As expected, the EDA  $\Delta E_{orb}$  is smaller when the partitioning is  
 343 performed from two quartet-prepared CH fragments. Also, and this shows very nicely the predic-  
 344 tivity of the EDA protocol, the minimum energy path for the association reaction is non-collinear,  
 345 proceeding via a trans configuration of the doublet CH moieties until at about a C-C distance  
 346 close to 1.35 Å an abrupt linearisation of the fragments occurs (see Fig. 5). A spatial decompo-  
 347 sition shows an interesting story (Supplementary Discussion 5). At about  $R_{\text{C-C}} = 2.6 \text{ \AA}$ , when  
 348 the CH fragments stop their free rotation adopting a clear trans geometry,  $E_{self}^{\text{CH}}$  suffers a rather  
 349 sudden increase, staying about 24 kcal mol<sup>-1</sup> above the isolated CH ground state energy for a  
 350 wide range of inter-fragment distances down to linearisation, where it grows again. This behavior  
 351 is clearly compatible with a quartet promotion. The figure also shows the contributions of the  
 352 doublet and quartet states for the (7,7) neutral fragment distribution, whose weight evolves from  
 353 1.0 at dissociation to about 0.4 at equilibrium. A comparison with dinitrogen, where the atomic  
 354 fragments are already in prepared quartets at dissociation, is also displayed. For acetylene, a sud-  
 355 den increase in the weight of the quartet is found coupled with the behavior of  $E_{self}^{\text{CH}}$ . As the Figure  
 356 shows, linearisation coincides with coalescence of the electron distribution probabilities over those  
 357 of dinitrogen. Thus, physically rigorous reference-less methods provide bonding models in agree-  
 358 ment with those of successful, yet heuristic approaches. They also helps us understand when, how,  
 359 and to what extent the use of fixed references will succeed or will be doomed to fail.

## References and dative bonding

Dative bonds break heterolytically, being usually weaker than electron-sharing ones, that break homolytically. However, as the  $C_2F_4$  and  $C_2H_2$  examples show, if the nature of the chemical interactions changes along the dissociation channel, it is in the end a set of EDA calculations with different fragment references which are used to decide between electron-sharing or donor-acceptor models. For instance, in the case of carbon suboxide,  $C_2O_3$ , the linear  $CO=C=CO$  model implies triplet CO fragments as well as a quintet carbon atom, a promotion that requires about 375 kcal mol<sup>-1</sup>, while the angular  $CO\rightarrow C\leftarrow CO$  one needs only exciting the C atom to its intra-configuration <sup>1</sup>D state, with a much lower cost of 29 kcal mol<sup>-1</sup>.<sup>53</sup> This points toward a promising role for reference-less methodologies in establishing the nature of dative bonding, that we illustrate with two systems.  $LiBe^+$  dissociates into <sup>1</sup>S  $Li^+$  and Be. In a SR calculation the charge of the Li atom is 0.946 au, with  $E_{int} = -30.2$  kcal mol<sup>-1</sup> dominated by a  $-21.0$  kcal mol<sup>-1</sup> charge-dipole  $V_{cl}$  term. The electron distribution has two main contributions,  $p(2,4) = 0.943$ ,  $p(3,3) = 0.054$ , so a bonding model emerges in which only one of the two valence electrons of Be delocalizes (Supplementary Discussion 6). It is important to consider the two electrons of a seemingly normal 2c,2e interaction independently. Using common spatial orbitals for them, as it is done in single or pseudo-single determinant approximations (e.g. in standard DFT) will mask an otherwise simple behavior, which is only recovered artificially (i.e the so-called left-right correlation) in multiconfigurational calculations or high-level valence bond approaches.<sup>54</sup> A simple solution is to use a (symmetry breaking) unrestricted single-determinant (UHF) ansatz. Fig. 6 shows that the two 2s electrons of Be in  $LiBe^+$  become spatially different at the UHF level: only one of the spatial orbitals delocalizes. A more interesting system is <sup>1</sup> $\Sigma^+$  BeO, which dissociates to ground state Be and <sup>1</sup>D excited O. MR data unveils how the interaction evolves from a donor-acceptor Be $\rightarrow$ O link to a very clear ionic-like regime. Since  $O^{2-}$  is not stable *in vacuo*, it is not possible to perform a standard EDA with charge-transfer  $Be^{2+}$  and  $O^{2-}$  references, a problem that doubtlessly biases interpretations. The BeO interaction (section S8) starts with an O atom displaying a kind of  $\sigma$ -hole, visible in the Laplacian of the density, which allows for a Be to O donor-acceptor  $\sigma$  favorable approach. The evolution of both the bond order, and particularly, the crystal clear behavior of  $E_{self}^{Be}$  evidence that as  $R$  decreases, a two step ionisation process occurs. In the first, similarly to what was found in  $LiBe^+$ , a Be electron is transferred to the oxygen. This is half completed at about  $R = 2.6$  Å, and at around 2.4 Å the second ionisation of Be starts. Simultaneously, already at 2.6 Å

391 two back-bonding  $\pi$  bonds involving the oxygen's electrons develop. Thanks to back-donation, at  
392 equilibrium,  $Q(\text{Be}) = 1.416$  e, although the Laplacian, for instance, shows quasi-spherical atomic  
393 shells. Also,  $p(2, 10) > 0.5$ . After the second ionisation starts, and surely at equilibrium, a better  
394 description of the system is that of an oxide anion donating rather symmetrically its  $\sigma$  and  $\pi$  elec-  
395 trons to a Be dication that acts as acceptor. In this regime, a dative, donor-acceptor bonding model  
396 is also admissible, but now the donor agent is the oxide anion.

397 Ubiquitous reference biases permeate the theory of chemical bonding, one of the pillars of  
398 modern chemistry. On the one hand, the internal references needed to interpret molecular wave-  
399 functions in terms of atomic (i.e. chemical) components, lead to the *interference* terms that lie at  
400 the root of the standard model of the chemical bond. On the other, most energy decomposition  
401 analyses, which become essential to discern among conflicting or alternative bonding images, rest  
402 on choosing external (energetic) references for the set of fragments that are meant to interact with  
403 each other. However, interacting fragments in-a-molecule are entities in *pseudo-mixed* quantum  
404 states, with fluctuating (i.e. not fixed) electron populations, electronic, and spin states. Failing to  
405 consider this fact leads to a variety of electron count or electron spin biases. The historical use of  
406 energy-promoted and/or spin-excited fragments to rationalize the nature of chemical links finds a  
407 rigorous conceptual root in considering fragments as open quantum systems. We have argued that  
408 real space analyses are as reference-less as possible, needing only the specification of a chemically  
409 sensible atomic partition of the space. If that ingredient is provided, no biases remain, and all the  
410 electron counts, electronic and spin states of the interacting fragments are part of the output, not  
411 of the input of the procedure. In this way, the best bonding model for a system is automatically  
412 read from the results of the analysis.

## 413 **Methods**

414 Electronic structure, QTAIM/IQA, and electron distribution calculations were performed with  
415 GAMESS<sup>55</sup>, PROMOLDEN<sup>56</sup>, and EDF<sup>57</sup>, respectively. All atomic charges and probabili-  
416 ties cited were obtained with QTAIM atoms. Details of calculations:  $\text{H}_2^+$ , FCI/cc-pVTZ;  $\text{H}_2$ ,  
417 CAS[2,2]//6-311G(p);  $\text{LiNa}^+$ , HF//6-311G(p,d)  $R_{eq} = 3.460$  Å;  $\text{He}_2^{2+}$ , FCI//cc-pVTZ,  $R_{eq} =$   
418  $1.332$  Å; LiF single reference, HF/def2-SVP,  $R_{eq} = 1.54$  Å; LiF multireference, MRCI-SD/d-  
419 aug-cc-pVDZ;  $\text{CH}_4$ ,  $\text{C}_2\text{H}_2$ , CASSCF/def2-TZVPP;  $\text{LiBe}^+$ , HF//6-311G(p),  $R_{eq} = 2.646$  Å, UHF  
420 also at the same geometry; BeO, CASSCF[8,8]/6-311G(p),  $R_{eq} = 1.345$  Å;

421 **Data Availability**

422 The data that support the findings of this study are available in the supporting information.

423 **Acknowledgements**

424 Financial support from the spanish MICINN, grant PGC2018-095953-B-I00 and the FICYT,  
425 grant IDI/2021/000054, is acknowledged.

426 **Author contributions**

427 E.F.M. and A.M.P. contributed equally to this work.

428 **Competing Interests**

429 The authors declare no competing interests

430 **Additional information**

431 The online version contains supplementary information available at xxxx

---

432 <sup>1</sup> Lewis, G. N. The atom and the molecule. *J. Am. Chem. Soc.* **38**, 762–786 (1916).

433 <sup>2</sup> Zhao, L., Pan, S., Holzmann, N., Schwerdtfeger, P. & Frenking, G. Chemical bonding and bonding  
434 models of main-group compounds. *Chem. Rev.* **119**, 8781–8845 (2019).

435 <sup>3</sup> Silvi, B. About lewis’s heritage: chemical interpretations and quantum chemistry. *Theor. Chem. Acc.*  
436 **136**, 1–6 (2017).

437 <sup>4</sup> Zhao, L., Schwarz, W. H. E. & Frenking, G. The lewis electron-pair bonding model: the physical  
438 background, one century later. *Nat. Rev. Chem.* **3**, 35–47 (2019).

439 <sup>5</sup> Zhao, L., Hermann, M., Schwarz, W. H. E. & Frenking, G. The lewis electron-pair bonding model:  
440 modern energy decomposition analysis. *Nat. Rev. Chem.* **3**, 48–63 (2019).

441 <sup>6</sup> Levine, D. S. & Head-Gordon, M. Clarifying the quantum mechanical origin of the covalent chemical  
442 bond. *Nat. Commun.* **11**, 1–8 (2020).

- 443 <sup>7</sup> Frenking, G. & Shaik, S. (eds.) *The chemical bond : fundamental aspects of chemical bonding* (Wiley-  
444 VCH Verlag, Weinheim, 2014).
- 445 <sup>8</sup> Mingos, D. M. P. *The chemical bond I : 100 years old and getting stronger* (Springer, Switzerland,  
446 2016).
- 447 <sup>9</sup> Hellmann, H. Zur rolle der kinetischen elektronenenergie für die zwischenatomaren kräfte. *Z. Phys.* **85**,  
448 180–190 (1933).
- 449 <sup>10</sup> Hellmann, H. *Einführung in die Quantenchemie* (Deuticke, Leipzig/Wien, 1937).
- 450 <sup>11</sup> Slater, J. C. The virial and molecular structure. *J. Chem. Phys.* **1**, 687–691 (1933).
- 451 <sup>12</sup> Feynman, R. P. Forces in molecules. *Phys. Rev.* **56**, 340–343 (1939).
- 452 <sup>13</sup> Shaik, S. *et al.* Quadruple bonding in c2 and analogous eight-valence electron species. *Nat. Chem.* **4**,  
453 195–200 (2012).
- 454 <sup>14</sup> Shaik, S., Rzepa, H. S. & Hoffmann, R. One molecule, two atoms, three views, four bonds? *Angew.*  
455 *Chem. Int. Ed.* **52**, 3020–3033 (2013).
- 456 <sup>15</sup> Frenking, G. & Hermann, M. Critical comments on “one molecule, two atoms, three views, four  
457 bonds?”. *Angew. Chem. Int. Ed.* **52**, 5922–5925 (2013).
- 458 <sup>16</sup> Ruedenberg, K. The physical nature of the chemical bond. *Rev. Mod. Phys.* **34**, 326–376 (1962).
- 459 <sup>17</sup> Schmidt, M. W., Ivanic, J. & Ruedenberg, K. Covalent bonds are created by the drive of electron waves  
460 to lower their kinetic energy through expansion. *J. Chem. Phys.* **140**, 204104 (2014).
- 461 <sup>18</sup> Ruedenberg, K. & Schmidt, M. W. Physical understanding through variational reasoning: Electron  
462 sharing and covalent bonding. *J. Phys. Chem. A* **113**, 1954–1968 (2009).
- 463 <sup>19</sup> Wilson, C. W. & Goddard, W. A. The role of kinetic energy in chemical binding. i. the nonclassical or  
464 exchange kinetic energy. *Theor. Chim. Acta* **26**, 195–210 (1972).
- 465 <sup>20</sup> Goddard, W. A. & Wilson, C. W. The role of kinetic energy in chemical binding. ii. contragradience.  
466 *Theor. Chim. Acta* **26**, 211–230 (1972).
- 467 <sup>21</sup> Bitter, T., Ruedenberg, K. & Schwarz, W. H. E. Toward a physical understanding of electron-sharing  
468 two-center bonds. i. general aspects. *J. Comput. Chem.* **28**, 411–422 (2006).
- 469 <sup>22</sup> Bitter, T., Wang, S. G., Ruedenberg, K. & Schwarz, W. H. E. Toward a physical understanding of  
470 electron-sharing two-center bonds. II. pseudo-potential based analysis of diatomic molecules. *Theor.*  
471 *Chem. Acc.* **127**, 237–257 (2010).
- 472 <sup>23</sup> Cardozo, T. M. & Nascimento, M. A. C. Chemical bonding in the n2 molecule and the role of the  
473 quantum mechanical interference effect. *J. Phys. Chem. A* **113**, 12541–12548 (2009).

- 474 <sup>24</sup> Fantuzzi, F. & Nascimento, M. A. C. Description of polar chemical bonds from the quantum mechanical  
475 interference perspective. *J. Chem. Theory Comput.* **10**, 2322–2332 (2014).
- 476 <sup>25</sup> Feynman, R. *The Feynman lectures on physics* (Basic Books, a member of the Perseus Books Group,  
477 New York, 2011).
- 478 <sup>26</sup> Bacskay, G. B. & Nordholm, S. Covalent bonding: The fundamental role of the kinetic energy. *J. Phys.*  
479 *Chem. A* **117**, 7946–7958 (2013).
- 480 <sup>27</sup> Nordholm, S. & Bacskay, G. B. The basics of covalent bonding in terms of energy and dynamics.  
481 *Molecules* **25**, 2667 (2020).
- 482 <sup>28</sup> Bader, R. F. W. *Atoms in Molecules* (Oxford University Press, 1990).
- 483 <sup>29</sup> Blanco, M. A., Martín Pendás, A. & Francisco, E. Interacting quantum atoms: A correlated energy  
484 decomposition scheme based on the quantum theory of atoms in molecules. *J. Chem. Theory Comput.*  
485 **1**, 1096–1109 (2005).
- 486 <sup>30</sup> Martín Pendás, A., Blanco, M. A. & Francisco, E. The nature of the hydrogen bond: A synthesis from  
487 the interacting quantum atoms picture. *J. Chem. Phys.* **125**, 184112 (2006).
- 488 <sup>31</sup> Guevara-Vela, J. M., Francisco, E., Rocha-Rinza, T. & Martín Pendás, A. Interacting quantum atoms—a  
489 review. *Molecules* **25**, 4028 (2020).
- 490 <sup>32</sup> Frenking, G. The physical origin of covalent bonding. In Frenking, G. & Shaik, S. (eds.) *The chemical*  
491 *bond : fundamental aspects of chemical bonding*, chap. 1 (Wiley-VCH Verlag, Weinheim, 2014).
- 492 <sup>33</sup> Ruedenberg, K. & Schmidt, M. W. Why does electron sharing lead to covalent bonding? a variational  
493 analysis. *J. Comput. Chem.* **28**, 391–410 (2006).
- 494 <sup>34</sup> Levine, D. S., Horn, P. R., Mao, Y. & Head-Gordon, M. Variational energy decomposition analysis  
495 of chemical bonding. 1. spin-pure analysis of single bonds. *J. Chem. Theory Comput.* **12**, 4812–4820  
496 (2016).
- 497 <sup>35</sup> Levine, D. S. & Head-Gordon, M. Quantifying the role of orbital contraction in chemical bonding. *J.*  
498 *Phys. Chem. Letters* **8**, 1967–1972 (2017).
- 499 <sup>36</sup> Levine, D. S. & Head-Gordon, M. Energy decomposition analysis of single bonds within kohn–sham  
500 density functional theory. *Proceedings of the National Academy of Sciences* **114**, 12649–12656 (2017).
- 501 <sup>37</sup> Martín Pendás, A., Francisco, E. & Blanco, M. A. An electron number distribution view of chemical  
502 bonds in real space. *Phys. Chem. Chem. Phys.* **9**, 1087–1092 (2007).
- 503 <sup>38</sup> Martín Pendás, A. & Francisco, E. Chemical bonding from the statistics of the electron distribution.  
504 *ChemPhysChem* **20**, 2722–2741 (2019).

- 505 <sup>39</sup> Martín Pendás, A., Francisco, E. & Blanco, M. Spatial localization, correlation, and statistical depen-  
506 dence of electrons in atomic domains: The  $x^1\sigma_g^+$  and  $b^3\sigma_u^+$  and states of  $\text{H}_2$ . *Chem. Phys. Letters* **437**,  
507 287–292 (2007).
- 508 <sup>40</sup> Martín Pendás, A., Francisco, E. & Blanco, M. A. Spin resolved electron number distribution functions:  
509 How spins couple in real space. *J. Chem. Phys.* **127**, 144103–1–144103–9 (2007).
- 510 <sup>41</sup> Francisco, E., Martín Pendás, A. & Blanco, M. A. A molecular energy decomposition scheme for atoms  
511 in molecules. *J. Chem. Theory Comput.* **2**, 90–102 (2005).
- 512 <sup>42</sup> Martín Pendás, A. & Francisco, E. Questioning the orbital picture of magnetic spin coupling: a real  
513 space alternative. *Phys. Chem. Chem. Phys.* **24**, 639–652 (2022).
- 514 <sup>43</sup> Ziegler, T. & Rauk, A. On the calculation of bonding energies by the hartree fock slater method. *Theor.*  
515 *Chim. Acta* **46**, 1–10 (1977).
- 516 <sup>44</sup> Mitoraj, M. P., Michalak, A. & Ziegler, T. A combined charge and energy decomposition scheme for  
517 bond analysis. *J. Chem. Theory Comput.* **5**, 962–975 (2009).
- 518 <sup>45</sup> Kraka, E., Zou, W. & Tao, Y. Decoding chemical information from vibrational spectroscopy data: Local  
519 vibrational mode theory. *WIREs Comput. Mol. Sci.* **10**, e1480 (2020).
- 520 <sup>46</sup> Zhao, L., Zhi, M. & Frenking, G. The strength of a chemical bond. *Int. J. Quant. Chem.* 1–9 (2021).
- 521 <sup>47</sup> Menéndez-Crespo, D., Costales, A., Francisco, E. & Martín Pendás, A. Real-space in situ bond energies:  
522 Toward a consistent energetic definition of bond strength. *Chem. Eur. J.* **24**, 9101–9112 (2018).
- 523 <sup>48</sup> Linstrom, P. Nist chemistry webbook, nist standard reference database 69 (1997).
- 524 <sup>49</sup> Andrada, D. M., Casals-Sainz, J. L., Martín Pendás, A. & Frenking, G. Dative and electron-sharing  
525 bonding in  $\text{C}_2\text{F}_4$ . *Chem. Eur. J.* **24**, 9083–9089 (2018).
- 526 <sup>50</sup> Jara-Cortés, J., Guevara-Vela, J. M., Martín Pendás, A. & Hernández-Trujillo, J. Chemical bonding in  
527 excited states: Energy transfer and charge redistribution from a real space perspective. *J. Comput. Chem.*  
528 **38**, 957–970 (2017).
- 529 <sup>51</sup> Casals-Sainz, J. L. *et al.* Exotic bonding regimes uncovered in excited states. *Chem. Eur. J.* **25**, 12169–  
530 12179 (2019).
- 531 <sup>52</sup> Seiler, P. & Dunitz, J. D. Are ionic solids really built of ions? new evidence from x-ray diffraction. *Helv.*  
532 *Chim. Acta* **69**, 1107–1112 (1986).
- 533 <sup>53</sup> Zhao, L., Hermann, M., Holzmann, N. & Frenking, G. Dative bonding in main group compounds.  
534 *Coord. Chem. Rev.* **344**, 163–204 (2017).
- 535 <sup>54</sup> Shaik, S. & Hiberty, P. C. *A chemist's guide to valence bond theory* (Wiley-Interscience, Hoboken, N.J,

- 536 2008).
- 537 <sup>55</sup> Barca, G. M. J. *et al.* Recent developments in the general atomic and molecular electronic structure  
538 system. *J. Chem. Phys.* **152**, 154102 (2020).
- 539 <sup>56</sup> Martín Pendás, A. & Francisco, E. Promolden: A QTAIM/IQA code (Available from the authors upon  
540 request by writing to [ampendas@uniovi.es](mailto:ampendas@uniovi.es)).
- 541 <sup>57</sup> Francisco, E., Martín Pendás, A. & Blanco, M. Edf: Computing electron number probability distribution  
542 functions in real space from molecular wave functions. *Comput. Phys. Commun.* **178**, 621 – 634 (2008).